Hindawi
Wireless Communications and Mobile Computing
Volume 2022, Article ID 7761150, 10 pages
https://doi.org/10.1155/2022/7761150

Research Article

A Low-Profile Compact Meander Line Telemetry Antenna with Low SAR for Medical Applications

N. H. Sulaiman,[1] **Muhammad Inam Abbasi**,[2] **N. A. Samsuri**,[3] **M. K. A. Rahim**,[3] **and F. C. Seman**[4]

[1]*School of Electrical Engineering and Artificial Intelligence, Xiamen University Malaysia, Sepang, Selangor, Malaysia*
[2]*Centre for Telecommunication Research & Innovation (CETRI), Faculty of Electrical and Electronic Engineering Technology (FTKEE), Universiti Teknikal Malaysia Melaka (UTeM), Melaka 76100, Malaysia*
[3]*School of Electrical, Faculty of Engineering, Universiti Teknologi Malaysia, 81310 Johor Bharu, Malaysia*
[4]*Fakulti Kejuruteraan Elektrik Dan Elektronik, Universiti Tun Hussein Onn Malaysia, 86400 Parit Raja, Batu Pahat, Johor, Malaysia*

Correspondence should be addressed to Muhammad Inam Abbasi; muhammad_inamabbasi@yahoo.com

Received 26 March 2022; Revised 26 July 2022; Accepted 30 July 2022; Published 12 August 2022

Academic Editor: Farman Ullah

A low-profile Compact Meander Line Telemetry Antenna (CMLTA) operating at 402.5 MHz for the Medical Implant Communication System (MICS) band medical applications is introduced. The proposed antenna focuses specifically on pacemaker telemetry applications. The meander line technique with an open loop configuration and simple transmission line feeding mechanism has been used for achieving the compact design. Based on the theory of surface current distribution, the proposed technique provides the opportunity to increase the electrical dimensions while decreasing the physical dimensions of the antenna. Further design optimization is carried out to optimize the overall antenna size to a maximum volume of 4080 mm^3. By introducing CMLTA, the size of the antenna is reduced by 79% as compared to the previous work. The proposed antenna demonstrated satisfactory performance with 10 dB bandwidth of 6.17%, a maximum gain of -22 dBi and an EIRP of -25.28 dBi. The analysis of Specific Absorption Rate under premise use of 1 W input power provided the maximum 1 g and averaged 10 g SAR of 74.7 W/kg and 17.7 W/kg, respectively, demonstrating a satisfactory level according to the IEEE standard safety guidelines. Fabrication and measurements are carried out where measured results are found to be in good agreement with the simulated results. With the optimized dimensions, satisfactory gain, EIRP, and SAR performance, the proposed CMLTA is deemed suitable for pacemaker telemetry applications for effective communication.

1. Introduction

The microstrip patch antennas are proposed by different researchers in various forms because of their compact size and high-performance capabilities. Many applications require high gain antennas, and hence, microstrip arrays are required for these applications [1–6], while other applications demand electrically small and compact antennas [7, 8]. The implantable antenna is one of its kind, which has been receiving immense attention nowadays [9–14]. Recent research works have shown that implantable antenna needs to be designed with broadband performance in order to reduce the shift in resonant frequency due to nonhomogenous human tissues [15]. The antenna size is one of the main issues in designing an implantable antenna. Besides that, maintaining good performance in different environments is indeed a challenging task. Some solutions have been suggested in the past, such as loading the ground plane with slots [16]. However, slotted ground design is confined to those applications without a conductor under the ground plane. Two more types of low-profile implantable antennas were introduced in [17], where spiral and PIFA structures were proposed to obtain a small size for implantable antennas. The radiation efficiency of PIFA was observed to be

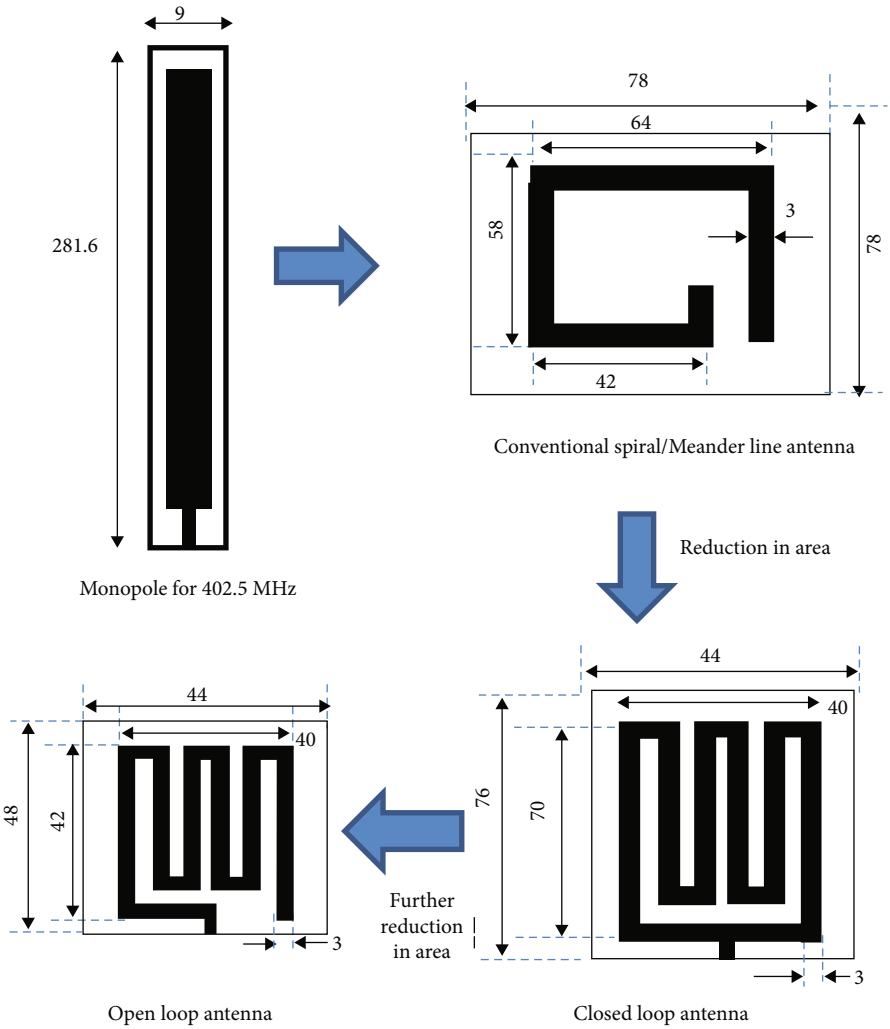

Figure 1: Detail design process and configuration of the proposed CMLTA (open loop) (all dimensions are in mm).

higher than that of the microstrip antenna. However, PIFA in [17] used high dielectric permittivity material to obtain a smaller size. In another work [18], an implantable antenna for pacemaker applications with dimensions of $42 \times 43.6 \times 11$ mm was proposed, and the investigations were carried out by implanting the antenna inside the pig. However, the accuracy of measured results and antenna size still remains the major issue to be resolved in implantable antenna design.

Since an implantable antenna has to be embedded in the human body, therefore, safety considerations have to be taken into account while designing such antennas. Moreover, the design process of biomedical systems involves Electromagnetic (EM) radiating structures like antennas, which might harm the human body by excessive exposure to radiation or thermal heating. Effective Isotropic Radiated Power (EIRP) is one of the factors that can be used to characterize and limit the radiated power from the antenna. The thermal heating of the tissues can be classified by the Specific Absorption Rate (SAR) [19, 20]. In order to preserve patient safety, the standard SAR guidelines need to be carefully addressed. The antenna is required to be designed with accuracy and carefulness, considering it is surrounded by a complicated tissue environment [21, 22]. Generally, for implantable antenna measurements and analysis, there are two approaches used to mimic the human body, which are the one-layer skin tissues model (homogenous phantom) and three-layer model (non-homogenous phantom) consisting of skin, fat, and muscle [23, 24]. In [25], two tissue models were compared, and the results showed that there is no significant discrepancy between the reflection coefficient of the antenna, while a slight resonant frequency shift was observed. In another work, the implantable antenna was also analyzed in the human body by using Gustav Voxel model, which is available in CST MWS [9]. This technique can also be useful, particularly for determining the antenna performance according to the safety limit for EIRP and SAR.

In this research work, an improved design of a low-profile implantable antenna based on the Compact Meander Line Telemetry Antenna (CMLTA) operating at 402.5 MHz for the Medical Implant Communication System (MICS) band medical applications is proposed. The antenna size has been reduced based on the optimization of the electrical length of the antenna, while the EIRP and SAR have been governed to follow the safety standards by the effective use

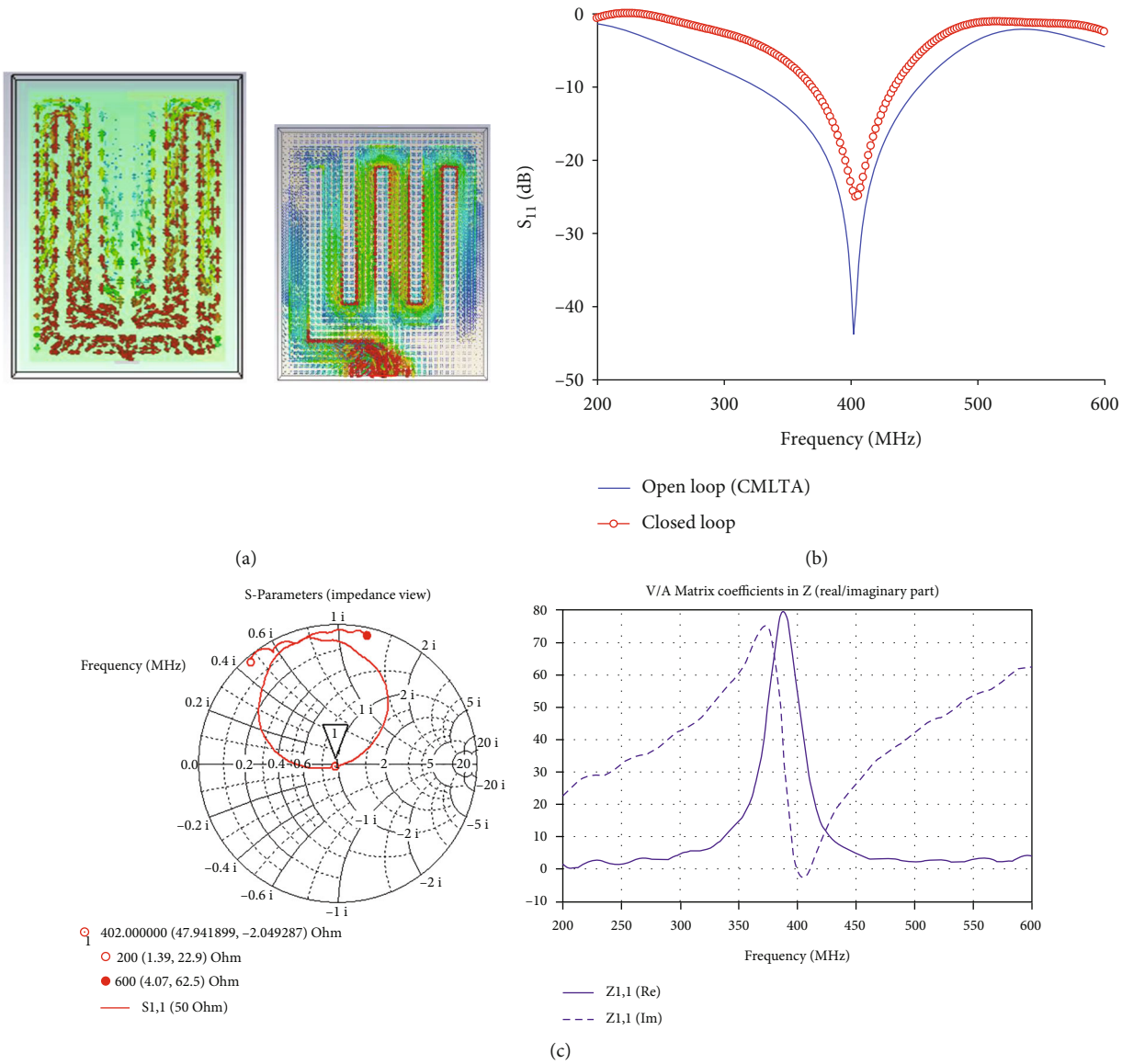

Figure 2: Comparison between closed loop and open loop (CMLTA): (a) surface current distribution; (b) simulated return loss performance; (c) wave impedance of the proposed CMLTA.

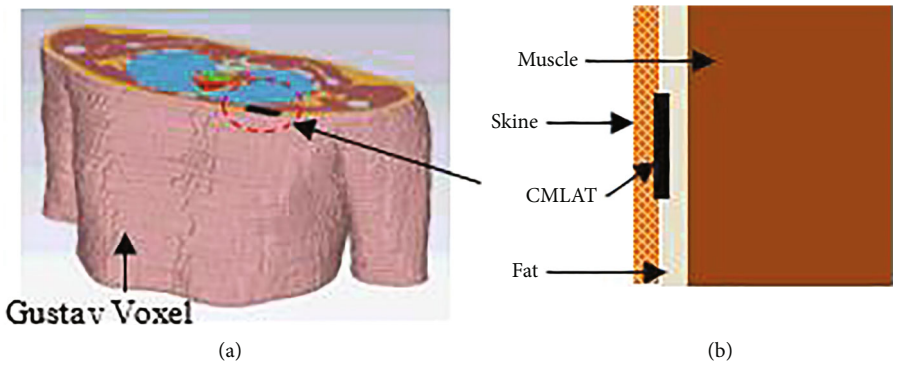

Figure 3: Simulations and measurements setup of the proposed antenna. (a) Simulation setup of the CMLTA in voxel body and (b) nonhomogenous phantom.

Table 1: Size comparison between the proposed antenna and previous work.

Ref.	References		Proposed CMLTA		Percentage reduction
	Design technique/material	Volume (mm^3)	Design technique	Volume (mm^3)	
[12]	PIFA/ Taconic CER-10 ($\varepsilon_r = 10$)	20143			79%
[11]	Microstrip Spiral/Rogers 3010 ($\varepsilon_r = 10.2$)	10240	Microstrip Meander Line/ ($FR\,4 = 4.7$ and $\tan\delta = 0.025$)	4080	60%
[11]	PIFA/Rogers 3010 ($\varepsilon_r = 10.2$)	6144			34%

of substrate and superstrate. The analysis is based on the measured results obtained using the developed single-layer homogeneous phantom model. The proposed CMLTA could be a suitable telemetry antenna to be implanted together with an artificial pacemaker.

2. Antenna Design and Optimization

The proposed antenna is designed at 402.5 MHz by means of commercially available CST Microwave Studio (CST MWS). Miniaturization of the implantable antenna is achieved by the optimization of the meander line technique as detailed in [26, 27]. Furthermore, open loop meander and closed loop meander line are also considered in the miniaturization process. The full ground plane configuration has been used, keeping in mind the requirements and sensitivity of the pacemaker telemetry applications. On the other hand, by introducing open loop configurations, the length and width of the substrate have been successfully reduced by 36.84% and 40%, respectively, as compared to the closed loop configuration. Design optimization of the antenna is carried out in order to achieve the optimum size and obtain efficient performance by comparing closed loop and open loop CMLTA, as shown in Figure 1.

The comparison between the surface current distribution and reflection coefficient performance of closed loop and open loop CMLTA antennas is shown in Figure 2(a). It can be observed from the figure that by implementing an open loop configuration, the surface current covers a longer distance, and hence, the electrical dimensions of the antenna are enlarged. This provides an opportunity to reduce the physical dimensions of the antenna. Figure 2(b) shows a comparison between the simulated return loss performance of open loop and closed loop meander line antennas. It has been demonstrated that open loop configuration offers higher bandwidth performance as compared to the closed loop configuration. Therefore, open loop configuration is chosen for further investigation in this work and annotated as Compact Meander Line Telemetry Antenna (CMLTA). Figure 2(c) shows the wave impedance of the proposed antenna, which was observed to be well matched at 402.5 MHz as in [28].

For further evaluation, the proposed CMLTA is also simulated in in-body environment. In this case, the CMLTA is added with the superstrate layer which is capable of protecting neighbouring body tissues surrounding the proposed

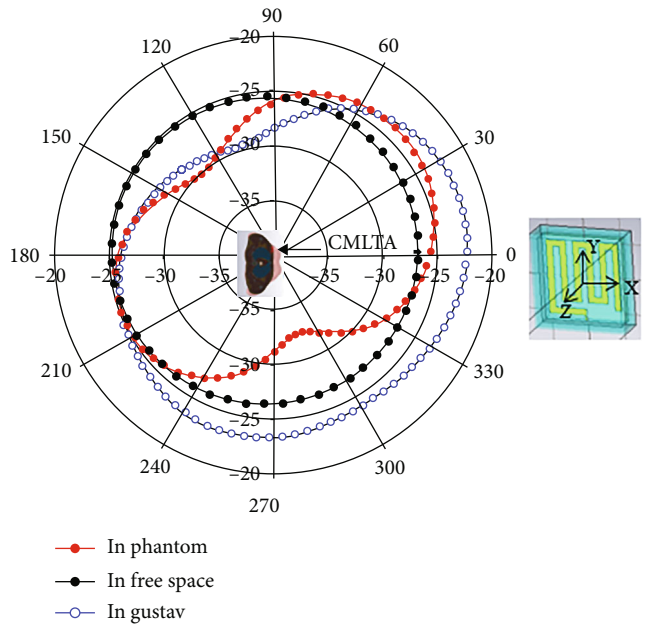

Figure 4: Simulated radiation patterns for CMLTA in phantom (nonhomogenous), Gustav voxel, and free space.

Table 2: G ain and EIRP of the proposed CMLTA.

Simulation environment	Peak gain (dBi)	Power (mW)	EIRP (dBm)
Homogeneous phantom	-24	0.745	-25.28
Nonhomogenous phantom	-29.9	0.110	-39.49
Gustav voxel	-22	0.085	-32.71

antenna. The superstrate layer acts as a buffer between the metal radiator and human tissues by reducing Radio Frequency (RF) power at the locations of lossy human tissues [29]. Therefore, for the proposed design, the superstrate and substrate have been used. In order to obtain a low profile antenna, FR-4 substrate has been chosen due to the low cost and easy fabrication. Based on the investigations carried out for different available thicknesses of FR4, 3.2 mm is observed to provide good matching, optimum size and better bandwidth performance as compared to other thicknesses of the superstrate. The complete assembly of the proposed antenna consists of a substrate with the full ground

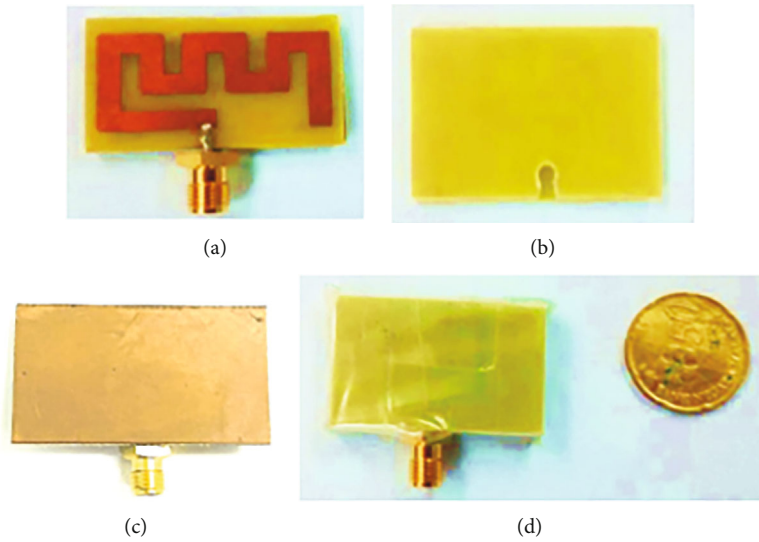

Figure 5: Fabricated antenna. (a) CMLTA on the substrate, (b) superstrate, (c) ground plane, and (d) CMLTA wrapped in plastic.

on one side and a radiating element on the other side. The radiating meander line is covered with the superstrate, and the antenna is placed inside the plastic casing. Different materials for the casing were investigated, which include plastic, aluminium, and tin, while the optimum desired performance was achieved by using plastic casing, as demonstrated in [30].

In order to investigate the performance of the proposed antenna inside the human body, simulations have been carried out in a nonhomogenous model as well as the Gustav body model made available by CST MWS as shown in Figure 3.

For the nonhomogenous model, the CMLTA is embedded under the skin and above fat and muscle layers. As in [31], the skin thickness is varied between 1 mm to 5 mm in order to observe its effect on the antenna performance. The size of the proposed antenna has been optimized by implanting the antenna inside the human body environment. However, for measurement purposes, the CMLTA has also been simulated in a homogenous phantom ($\varepsilon_r = 59.95$, $\tan\delta = 0.622$). The size comparison of the proposed antenna with previous work is shown in Table 1, while the radiation pattern of the antenna is shown in Figure 4.

It can be observed that a good monopole-like far-field pattern can be achieved by the proposed antenna design. The maximum realized gains at 402.5 MHz in nonhomogenous phantom and Gustav voxel are -24 dBi and -22 dBi, respectively, which are considered suitable for pacemaker telemetry applications. Based on the IEEE guidelines for safety, the EIRP of the implantable antenna should be lesser than -16 dBm [31]. The EIRP of the proposed design is -25.28 dBm and -32.71 dBm for homogeneous phantom and Gustav voxel, as shown in Table 2.

3. Fabrication and Measurements

The Compact Meander Line Telemetry Antenna (CMLTA) has been fabricated using 3.2 mm thick FR-4 ($\varepsilon_r = 4.7$, $\tan\delta = 0.025$) dielectric substrate (both for substrate and superstrate). The width (Ws) and length (Ls) of the substrate are 30 mm and 21.25 mm, respectively. As discussed in a previous work [32], the implantable antenna has to be protected using a casing in order to avoid direct contact with the developed phantom. The proposed antenna has to be wrapped in plastic for measurement purposes so that the radiating element can be covered and direct contact with the liquid phantom can be avoided. If the wrapping is not proper, it will affect the RF signal; hence, the CMLTA performance will be degraded. The fabricated sample of the proposed CMLTA is shown in Figure 5.

For measurement purposes, the homogenous liquid phantom has been successfully developed using the composition of water (51.3%), sugar (47.3%), and salt (1.4%) to achieve phantom properties at 402.5 MHz. Various composite samples of

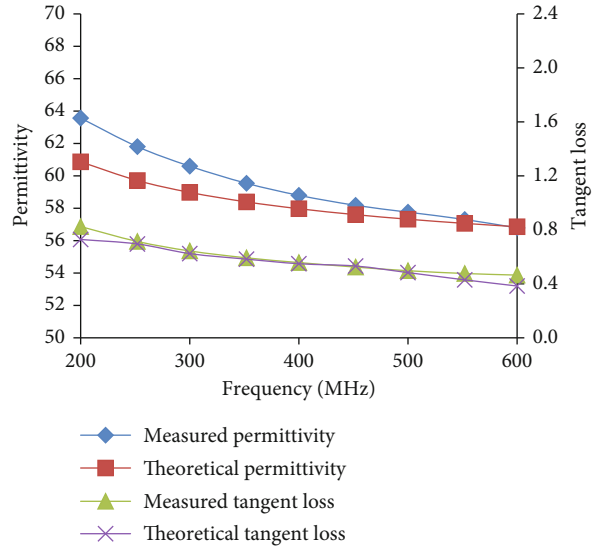

Figure 6: Comparison between measured and theoretical material properties of the developed phantom.

Figure 7: Measurement setup of CMLTA in a homogeneous phantom.

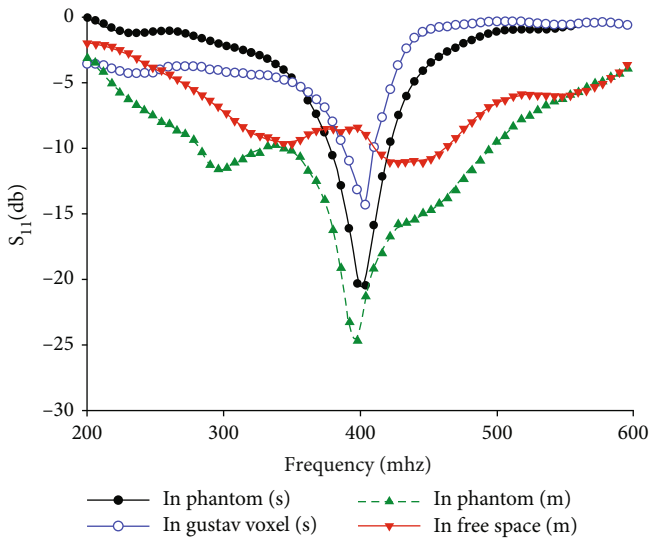

Figure 8: Simulated (s) and measured (m) CMLTA performances.It can be observed that the measured results are in good agreement with the simulated results, especially in the case of the phantom model. It can also be noted that the proposed implantable antenna worked well within the MICS band (402 MHz-405 MHz). The antenna in free space demonstrated a shift in resonant frequency as expected as the proposed antenna is purposely designed to be utilized in an in-body environment.

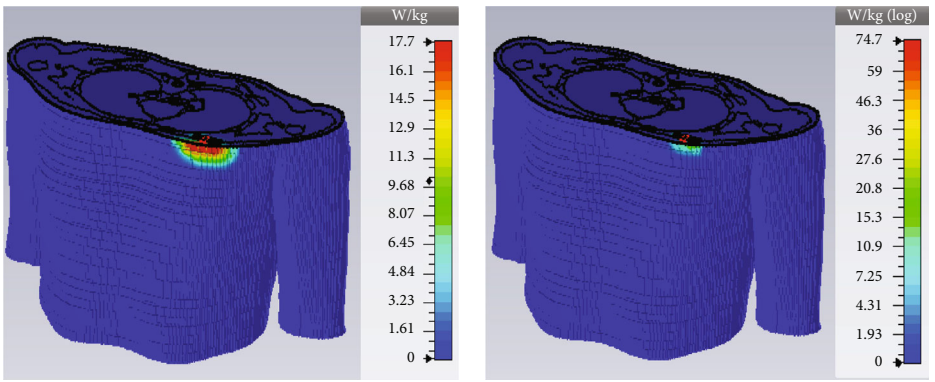

(a) 10 g (b) 1 g

Figure 9: SAR distribution in Gustav model at 402.5 MHz (1 W input power).

Table 3: SAR of CMLTA.

Standard	Maximum SAR (W/kg)	Maximum input power (mW)
C95.1-1999 (1 g-avg)	74.7	8.31
C95.1-2005 (10 g-avg)	17.7	55.20

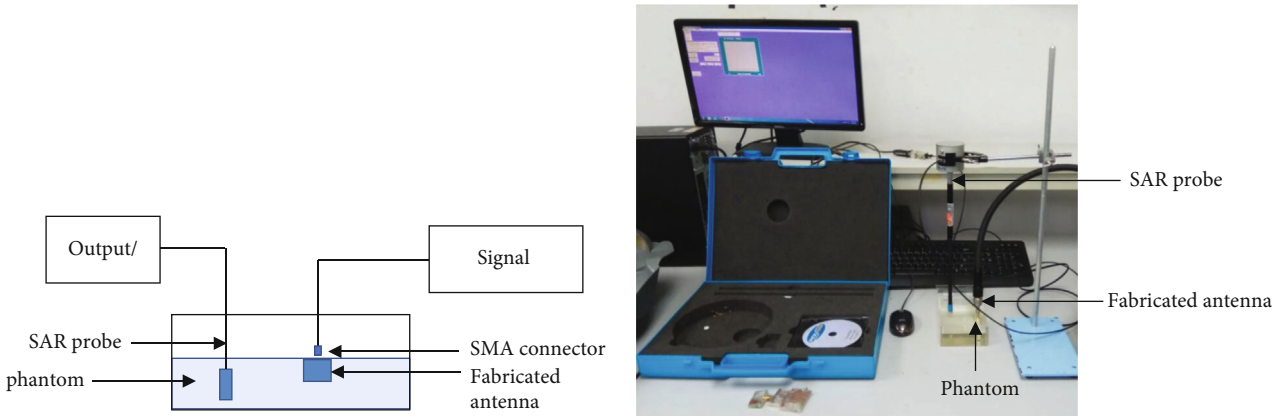

Figure 10: SAR measurements: (a) general measurement setup; (b) SAR measurements using liquid phantom.

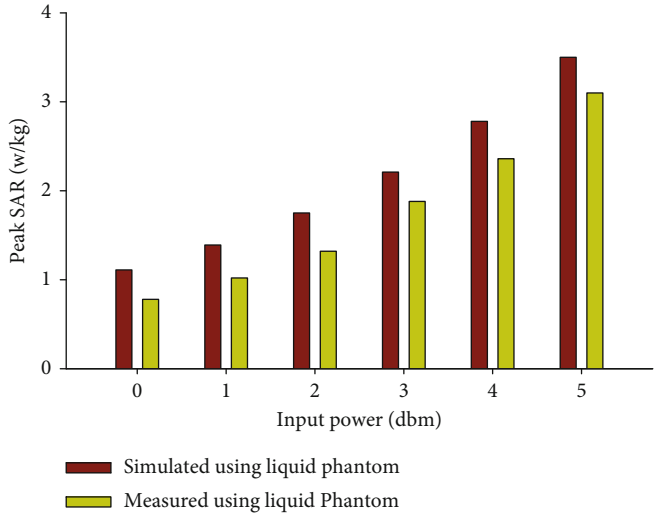

Figure 11: Simulated and measured SAR using liquid phantom.

Table 4: Performance comparisons of the proposed antenna and other implantable antennas.

Ref.	10 dB-BW (%)	Implantation tissue	Peak gain (dBi)	1 g-avg max SAR (W/kg)
[36]	8.37	Skin	—	294
[37]	5.17	Muscle	—	274.9
[38]	6.09	Skin	-33.2	606
CMLTA	6.17	Voxel body	-22	74.7

the solution have been developed to characterize material properties for comparison with the theoretical properties at 402.5 MHz [17]. Figure 6 shows the optimum dielectric properties achieved from the developed solution. The measured dielectric properties of the proposed solution have good agreement with theoretical values provided by FCC, with a maximum discrepancy of 0.43% in permittivity and 11.11% in conductivity. The obtained measured results are much closer to the FCC [33] values as compared to the results provided in the previously proposed phantom [34].

By using the developed phantom $S_{11,}$ measurements of the CMLTA have been carried out with a Vector Network

Analyzer (VNA). The measurement setup is shown in Figure 7.

As depicted in Figure 7, the CMLTA, wrapped in plastic, has been completely immersed in the developed liquid phantom. Moreover, it has been assured that the SMA connector is not having any contact with the phantom, which can modify the input impedance and hence can provide improper measured results. The comparison between the measured and simulated results is shown in Figure 8.

4. Specific Absorption Rate Analysis

In the simulation, the CMLTA is placed inside the Gustav body model, which consists of multiple layers of tissues such as muscle, skin, and fat. The CMLTA is implanted in between the skin tissue and muscle. The input power of 1 W is used, and the SAR distribution is as shown in Figure 9.

The maximum SAR is observed near the skin. No further penetration is observed as the CMLTA is equipped with a superstrate layer that protects the adjacent body tissue. Based on the previous studies, SAR investigations have also been carried out using 1 W as input power [35]. Under the premise of 1 W input power, the maximum of 10 g and 1 g average of SAR is 74.7 W/kg and 17.7 W/kg, respectively. Hence, to meet the 1 g and 10 g IEEE standards, the allowed input power of the CMLTA should be limited to 8.31 mW and 55.20 mW, respectively. The tabulated SAR results are shown in Table 3. In addition, the results are also recorded for different input power ranging from 0 dBm to 5 dBm (as the range of power is considered in [20]).

In order to validate the simulations, measurements are conducted, and the measurement setup for SAR is shown in Figure 10. The SAR probe from INDEXSAR is used to measure SAR using the *CheckSar* software interface. The fabricated CMLTA is connected to the signal generator. The CMLTA is immersed in the developed liquid phantom, and the input power is varied as in the simulation. The graphical results for SAR measurements and comparison with simulations for variable input power are shown in Figure 11.

It can be observed from Figure 11 that by varying input power from 0 dBm to 5 dBm, peak SAR has increased from 1.11 W/kg to 3.50 W/kg. The increment of peak SAR follows the theoretical trend of SAR, where a higher SAR level is distributed with higher excited power due to more absorption of energy by the human body.

Table 4 outlines the performance comparison of the proposed CMLTA to different implantable antennas. It can be seen that the CMLTA offers 6.17% of bandwidth performance, which is in the same range as previous works. Moreover, in this work, peak gain and SAR performance have also been compared between voxel body and phantom muscles demonstrating much better SAR performance.

5. Conclusions

A Compact Meander Line Antenna (CMLTA) has been designed and developed for implantable medical applications. By employing the meander line technique, a CMLTA has been proposed where the overall dimensions have provided a 79% reduction as compared to the antenna designs provided by the previous researchers. Moreover, CMLTA is easier to fabricate and has a low-cost antenna. A homogenous phantom has also been developed for validation through measurements. The reflection coefficient or S_{11} is successfully investigated by using a developed phantom, and a peak gain of -22 dBi with an EIRP of -25.28 dBi is demonstrated. Moreover, SAR analysis of the proposed antenna is carried out where the maximum SAR value is observed to be 74.7 W/kg which satisfies the IEEE standard safety guidelines. In the future, the antenna will be further used for In-Vivo measurements in order to demonstrate its applicability in implantable medical applications.

Data Availability

Data can be obtained by contacting the corresponding author.

Conflicts of Interest

The authors declare no conflict of interest.

Acknowledgments

This research was funded by MyBrain15 and Universiti Teknologi Malaysia (UTM) grant numbers 12H08 and 4F883. The authors are also thankful to the Centre for Research and Innovation Management (CRIM), Universiti Teknikal Malaysia Melaka (UTeM), for the financial support of this work.

References

[1] M. Alibakhshikenari, B. S. Virdee, P. Shukla et al., "Metamaterial-Inspired antenna array for application in microwave breast imaging systems for tumor detection," *IEEE Access*, vol. 8, pp. 174667–174678, 2020.

[2] M. Alibakhshikenari, B. S. Virdee, and E. Limiti, "Study on isolation and radiation behaviours of a 34×34 array-antennas based on SIW and metasurface properties for applications in terahertz band over 125-300 GHz," *Optik*, vol. 206, article 163222, 2020.

[3] M. Alibakhshikenari, B. S. Virdee, A. A. Althuwayb et al., "Study on on-chip antenna design based on metamaterial-inspired and substrate-integrated waveguide properties for millimetre-wave and THz integrated-circuit applications," *Journal of Infrared, Millimeter, and Terahertz Waves*, vol. 42, no. 1, pp. 17–28, 2021.

[4] A. Y. I. Ashyap, S. Alamri, S. H. Dahlan et al., "Triple-band metamaterial inspired antenna for future terahertz (THz) applications," *Computers, Materials & Continua*, vol. 72, no. 1, pp. 1071–1087, 2022.

[5] M. Inam, M. H. Dahri, M. H. Jamaluddin, N. Seman, M. R. Kamarudin, and N. H. Sulaiman, "Design and characterization of millimeter wave planar reflectarray antenna for 5G communication systems," *Engineering*, vol. 29, no. 9, article e21804, 2019.

[6] M. Inam and M. Y. Ismail, "Integration of PIN diodes with slot embedded patch elements for active reflectarray antenna

design," in *2012 International Symposium on Telecommunication Technologies*, Kuala Lumpur, Malaysia, 2012.

[7] R. Patel and T. Upadhyaya, "Electrically small inverted L planar patch antenna for wireless application," *Microwave and Optical Technology Letters*, vol. 60, no. 10, pp. 2351–2357, 2018.

[8] R. Patel and T. Upadhyaya, "An electrically small antenna for nearfield biomedical applications," *Microwave and Optical Technology Letters*, vol. 60, no. 3, pp. 556–561, 2018.

[9] L. Berkelmann and D. Manteuffel, "Antenna parameters for on-body communications with wearable and implantable antennas," *IEEE Transactions on Antennas and Propagation*, vol. 69, no. 9, pp. 5377–5387, 2021.

[10] Y. Feng, Y. Li, L. Li, B. Ma, H. Hao, and L. Li, "Design and system verification of reconfigurable matching circuits for implantable antennas in tissues with broad permittivity range," *IEEE Transactions on Antennas and Propagation*, vol. 68, no. 6, pp. 4955–4960, 2020.

[11] F. Faisal, M. Zada, A. Ejaz, Y. Amin, S. Ullah, and H. Yoo, "A miniaturized dual-band implantable antenna system for medical applications," *IEEE Transactions on Antennas and Propagation*, vol. 68, no. 2, pp. 1161–1165, 2020.

[12] C. Liu, Y. Zhang, and X. Liu, "Circularly polarized implantable antenna for 915 MHz ISM-band far-field wireless power transmission," *IEEE Antennas and Wireless Propagation Letters*, vol. 17, no. 3, pp. 373–376, 2018.

[13] H. Li, B. Wang, L. Guo, and J. Xiong, "Efficient and wideband implantable antenna based on magnetic structures," *IEEE Transactions on Antennas and Propagation*, vol. 67, no. 12, pp. 7242–7251, 2019.

[14] I. A. Shah, M. Zada, and H. Yoo, "Design and analysis of a compact-sized multiband spiral-shaped implantable antenna for scalp implantable and leadless pacemaker systems," *IEEE Transactions on Antennas and Propagation*, vol. 67, no. 6, pp. 4230–4234, 2019.

[15] O. H. Murphy, A. Borghi, M. R. Bahmanyar et al., "RF communication with implantable wireless device: effects of beating heart on performance of miniature antenna," *Healthcare Technology Letters*, vol. 1, no. 2, pp. 51–55, 2014.

[16] C. Liu, S. Member, Y. Guo, S. Member, and S. Xiao, "A hybrid patch/slot implantable antenna for biotelemetry devices," *IEEE Antennas and Wireless Propagation Letters*, vol. 11, pp. 1646–1649, 2013.

[17] J. Kim and Y. Rahmat-Samii, "Implanted antennas inside a human body: simulations, designs, and characterizations," *IEEE Transactions on Microwave Theory and Techniques*, vol. 52, no. 8, pp. 1934–1943, 2004.

[18] U. Kim and J. Choi, "An implantable antenna for wireless body area network application," *Journal of Electromagnetic Engineering and Science*, vol. 10, no. 4, pp. 206–211, 2010.

[19] K. Agarwal and Y. Guo, "Interaction of electromagnetic waves with humans in wearable and biomedical implant antennas," in *2015 Asia-Pacific Symposium on Electromagnetic Compatibility (APEMC)*, pp. 154–157, Taipei, Taiwan, 2015.

[20] A. Kiourti and K. S. Nikita, "Detuning issues and performance of a novel implantable antenna for telemetry applications," in *2012 6th European Conference on Antennas and Propagation (EUCAP)*, pp. 746–749, Prague, Czech Republic, 2011.

[21] C. Liu, S. Member, Y. Guo, S. Member, and H. Sun, "Design and safety considerations of an implantable rectenna for far-field wireless power transfer," *IEEE Transactions on Antennas and Propagation*, vol. 62, no. 11, pp. 5798–5806, 2014.

[22] N. Othman, N. Asmawati, and N. Akma, "Evaluation of specific absorption rate due to medical implant in near-field exposure," *Jurnal Teknologi*, vol. 64, no. 3, pp. 23–27, 2013.

[23] N. A. Samsuri and J. A. Flint, "A study on the effect of loop-like jewellery items worn on human hand on Specific Absorption Rate (SAR) at 1900 MHZ," in *2008 Loughborough Antennas and Propagation Conference*, pp. 297–300, Loughborough, UK, 2008.

[24] E. Rajo-iglesias, "A review of implantable patch antennas for biomedical telemetry: challenges and solutions [wireless corner]," *IEEE Antennas and Propagation Magazine*, vol. 54, no. 3, pp. 210–228, 2012.

[25] A. Kiourti and K. S. Nikita, "Accelerated design of optimized implantable antennas for medical telemetry," *IEEE Antennas and Wireless Propagation Letters*, vol. 11, pp. 1655–1658, 2012.

[26] N. H. Sulaiman, N. A. Samsuri, M. K. A. Rahim, F. C. Seman, and M. Inam, "Compact meander line telemetry antenna for implantable pacemaker applications," *Indonesian Journal of Electrical Engineering and Computer Science*, vol. 10, no. 3, p. 883, 2018.

[27] N. H. Sulaiman, N. A. Samsuri, M. K. A. Rahim, F. C. Seman, and M. Inam, "Design and analysis of optimum performance pacemaker telemetry antenna," *Telekomnika*, vol. 15, no. 2, p. 877, 2017.

[28] I. Kim, S.-G. Lee, Y.-H. Nam, and J.-H. Lee, "Investigation on wireless link for medical telemetry including impedance matching of implanted antennas," *Sensors*, vol. 21, no. 4, article 1431, 2021.

[29] H. Li, Y. X. Guo, C. Liu, S. Xiao, and L. Li, "A miniature-implantable antenna for medradio-band biomedical telemetry," *IEEE Antennas and Wireless Propagation Letters*, vol. 14, pp. 1176–1179, 2015.

[30] E. Hanada, Y. Antoku, S. Tani et al., "Electromagnetic interference on medical equipment by low-power mobile telecommunication systems," *IEEE Transactions on Electromagnetic Compatibility*, vol. 42, no. 4, pp. 470–476, 2000.

[31] Z. Duan, Y. X. Guo, M. Je, and D. L. Kwong, "Design and in vitro test of a differentially fed dual-band implantable antenna operating at MICS and ISM bands," *IEEE Transactions on Antennas and Propagation*, vol. 62, no. 5, pp. 2430–2439, 2014.

[32] A. M. A. Waddah, N. R. Khairun, and M. S. Abdirahman, "Performance of ultra-wideband wearable antenna under severe environmental conditions and specific absorption rate (Sar) study at near distances," *ARPN Journal of Engineering and Applied Science*, vol. 10, no. 4, pp. 1613–1622, 2015.

[33] FC Commission, D. L. Means, and K. W. Chan, *Evaluating compliance with FCC guidelines for human exposure to radio-frequency electromagnetic fields supplement C, edition 01-01-OET bulletin 65, edition 97-01*, Federal Communications Commission, Washington, D. C., 2001.

[34] C. Liu, Y. X. Guo, and S. Xiao, "Compact dual-band antenna for implantable devices," *IEEE Antennas and Wireless Propagation Letters*, vol. 11, pp. 1508–1511, 2012.

[35] S. Sabrin, K. P. Esselle, and K. M. Morshed, "A compact implantable antenna for bio-telemetry," in *2015 International Symposium on Antennas and Propagation (ISAP)*, pp. 2–5, Hobart, TAS, Australia, 2015.

[36] J. Kim and Y. Rahmat-samii, "Planar inverted-F antennas on implantable medical devices: meandered type versus spiral type," *Microwave and Optical Technology Letters*, vol. 48, no. 3, pp. 567–572, 2006.

[37] W. Huang and A. A. Kishk, "Embedded spiral microstrip implantable antenna," *International Journal of Antennas and Propagation*, vol. 2011, Article ID 919821, 6 pages, 2011.

[38] R. Li and S. Xiao, "Compact slotted semi-circular antenna for implantable medical devices," *Electronics Letters*, vol. 50, no. 23, pp. 1675–1677, 2014.